EUROVOLC

European Network of
Observatories and Research Infrastructure for Volcanology

Deliverable Report

D22.1: Retrieval algorithms for volcanic ash characterization

Work Package:	*Tools and techniques for rapid characterization of volcanic plumes*	
Work Package number:	*WP22*	
Work Package leader:	*Barbara Brooks*	
Task (Activity) name:	*Retrieval algorithms for volcanic ash characterisation*	
Task number:	*D22.1*	
Responsible Activity leader:	*Barbara Brooks*	
Lead beneficiary:	*5 - UNILEEDS*	
Author(s)	*Barbara Brooks*	
Type of Deliverable:	*Report [X]* *Prototype [ ]*	*Demonstrator [ ]* *Other [ ]*
Dissemination level:	*Public [X]* *Prog. Participants [ ]*	*Restricted Designated Group [ ]* *Confidential (consortium) [ ]*

Programme: H2020
Project number: 731070

Summary

This report details progress towards the development of an operation algorithm that will identify aerosol layers and the microphysical properties of the particulates within the layer. The system is designed around the current lidar remote sensing capabilities of the Icelandic and UK Meteorological Offices and the UK's National Centre for Atmospheric Science but in principle can be expanded to include other remote sensing techniques specifically radiometry.

The rational for why this is needed is provided addition to the formulation of the core problem. Due to this being an inversion problem that is mathematically ill-posed there is no exact solution and as a consequence a wide variety of methodologies that are scenario and instrument specific have been developed: many of the spurred on by the disruption caused by the Eyjafjallajökull eruption. A brief tour of those considered most promisings are introduced.

The results so far show the conceptual structure of methodology to be adopted here and how it depends on modules to feed information to it. The proposed methodology requires input from measurements hence to maximise efficiency and ensure transparency documented standard operating procedures for instrument operation and data processing have been, or are being, developed. The current standing is that the computational environment required to develop an appropriate single particle optical properties data set and to develop the forward model are being gathered together while the automated measurement processing software is being optimized and generalised. All modules are being designed to operate in a python environment and without the need for preparatory add-ons.

Introduction

During times of volcanic eruption the hazard posed by ash is evident: for example the risk to aviation through ingestion of ash into engines and abrasion providing pathways for attack by corrosive gases, while there is a very present risk in the near field to health and infrastructure through ash deposition and secondary surface transport. The hazard and risk posed by volcanic ash extends beyond the eruptive period due to the possibility of re-suspension with surface conditions (snow and vegetation cover, surface winds and moisture) being the major drivers determining the amount and height to which surface ash\dust is lofted: high winds are needed to loft ash\dust to heights that impact on aviation but only relatively low winds are required to move substantial volumes of ash\dust and to loft ash\dust at low levels (less than 10m) where it poses a risk to plant, animal and human health as well as to transport infrastructure. The re-suspension and transport of ash\dust is not however entirely negative as significant improvement to soil fertility can result.

It is worth discussing at this point the distinction between ash, volcanic ash, and dust. The term ash is usually used in reference to particulates resulting from combustion processes and as such is carbon rich. This is in contrast to volcanic ash which, as the name suggests, results from volcanic emissions and is silicone rich. Once volcanic ash is deposited it begins to age through weathering and once over 2 years old is referred to as dust (more directly once it has been exposed to snow cover during winter). The term dust also refers to the particulate matter arising from glacial erosion and also that due to the erosion and aeolian transport of sand and soil. Generically the aerosol loading in times of volcanic inactivity will be a mixture of dust (volcanic in origin or otherwise), sea-salt (in a marine environment such as the Icelandic coast), sulphate aerosol (sea-salt and none sea-salt in origin), and a wide range of other aerosol both natural and anthropogenic in origin.

The Volcanic Ash Advisory Centres (VAACs) are responsible for monitoring and forecasting the movement of volcanic ash\dust when the ash\dust concerned poses a risk to aviation. When the advisory is with regard to re-suspension events there is no discrimination as to the source of the material and so the worst case scenario is assumed (particulate matter is volcanic in origin). The advisories are only issued when there is any risk to aviation so there exists instances when substantial low level lofting occurs that poses risk on a local civil contingency basis.

The advisories issued include multi-level concentration maps that are the result of dispersion modelling. The most common dispersion models used are NAME, FALL3D, and HYSPLIT:

- NAME is a Lagrangian advection-diffusion model (Jones et al., 2007). Model particles are advected by 3D wind fields and dispersed using random walk techniques. NAME includes parameterizations of small-scale atmospheric turbulence and unresolved mesoscale motions, and accounts for sedimentation, as well as wet and dry deposition processes. It can be used with a range of different NWP meteorological datasets including output from the Global configuration of the Unified Model (UM) and ECMWF data.
- FALL3D is a 3-Dimensional time-dependent Eulerian model developed and maintained by INGV and the Barcelona Super Computer Centre (Costa et al., 2006). The model solves a set of advection-diffusion-sedimentation (ADS) equations on a structured terrain-following grid using a second-order Finite Differences (FD) explicit scheme. It can be used with a range of different NWP meteorological datasets,

at the global (e.g. GFS), mesoscale (e.g. WRF) and urban scale (e.g. CALMET). Several parameterizations can be chosen to describe particle terminal settling velocity and eddy diffusivity tensor. The eruption source is also flexible: the different source geometries which can be applied include *point*, *Suzuki*, and *top hat*.

- HYSPLIT is a hybrid Lagrangian / Eulerian model developed and maintained by NOAA (Stein et al. 2015). It supports multiple meteorological datasets, but data needs to be in ARL (a HYSPLIT specific) format and typically GFS is used. The user can choose from a number of turbulence schemes and wet and dry deposition schemes, and the particle characteristics can be defined (their diameter, shape and density), however only point or line sources are supported.

All the models require initialisation: that is starting state information. During eruptions the vital information includes plume height, mass ejection rate, particle density and particle size distribution (PSD) while for the latter two are essential for cases of re-suspension. In both cases meteorological information is required but that is sourced from ECMWF, GSF or WRF model output.

The most common remote sensing observing systems are radar, lidar, and lidar-ceilometer based which may be supplemented by the addition of a photometer. Both the Icelandic Meteorological Office (IMO) and the UK's National Centre for Atmospheric Science (NCAS) are developing mobile observatories for both Icelandic volcano monitoring and civil contingency support. Both observatories have 1550 nm wavelength scanning lidar with depolarisation channels and a 905 nm wavelength lidar-ceilometer. The UK Met Office (UKMO) have also installed a lidar\photometer network around the UK specifically to monitor ash, volcanic ash and dust but this does not operate 24/7: rather it is only activated during periods interest.

The goal of this part of WP22 is to develop a number of retrieval algorithms that can be used operationally both during times of volcanic unrest and in a civil contingency capacity during times of quiescence. That is a system that can deliver in near real time (no more than 10 minute delay) 5 - 10 minute averages of particle size distribution (PSD), can discriminate and segregate into recognised geophysical categories (Mereu et al., 2108, Omar et al., 2009) and has the flexibility to allow the integration of addition remote sensing data (e.g. radar, sun-photometer) as and when available.

What is the problem?

A monostatic, single-wavelength pulsed lidar system emits short laser pulses in to the atmosphere and measures the amount of light backscattered into a telescope as a function of distance. For a non-absorbing scattering atmosphere the relationship between single scattered light and the particulate loading in the measurement volume is given by the lidar equation (Kovalev and Eichinger, 2004):

$$P(z) = C_0 \frac{\beta_\lambda(z)}{z^2} exp\left[-2\int_0^z \alpha_\lambda(x)dx\right] \quad 1$$

where P(z) is instantaneous power of the analogue signal at the lidar photodetector output created by the singly scattered light from a scattering particle at range z. $\beta_\lambda(z)$ is the total (molecular and particulate) backscattering coefficient at the laser wavelength λ and $\alpha_\lambda(z)$ is the total extinction coefficient. The factor C_0 is the lidar system constant.

The backscattering coefficient describes the scattering strength in to the direction of the receiving telescope and is dependent on the wavelength of the incident light, type, shape, sized and PSD of the scatterers. The extinction coefficient is a description of the absorption and scattering capabilities of the scatterers in the volume at the wavelength of the incident light.

Elastic backscatter lidar systems do not allow for a separate measurement of $\beta_\lambda(z)$ and $\alpha_\lambda(z)$ as two unknowns cannot be determined with one measured variable. For calibrated lidar systems (including ceilometers), as used by IMO, NCAS, and UKMO a convenient parameter to work with is the attenuated backscatter coefficient, $\gamma_\lambda(z)$, which is relates to $\beta_\lambda(z)$ by (Geisinger et al., 2017):

$$\gamma_\lambda(z) = \beta_\lambda(z)\left(-2\int_0^z \alpha_\lambda(x)dx\right) \quad 2$$

At the wavelength used by the lidar systems providing the data, 1550 nm (scanning lidar) and 905 nm (ceilometer) the contribution to the total backscatter and extinction coefficients from molecules in negligible: it is particle scattering that is the dominant process. The link between the measured coefficients and the physical scattering process comes in the form of extinction coefficients: these are the ratios between the optical and physical cross-sections. Where there are N scatters of radius r in the scattering volume at range z then the backscatter and extinction coefficients are given by (van de Hulst, 1981):

$$\beta_\lambda(z) = N\pi r^2 Q_{bck} \quad 3$$

$$\alpha_\lambda(z) = N\pi r^2 Q_{ext} \quad 4$$

where Q_{bck} and Q_{ext} are the single particle backscatter and extinction efficiencies respectively and N is the number of particles of radius r.

In reality the particulate population in the scattering volume will be an ensemble of particles of different sizes described by a PSD dN/dr in which case equation 3 and 4 can be rewritten as:

$$\beta_\lambda(z) = \int_0^\infty \frac{dN}{dr} \pi r^2 Q_{bck} dr \quad 5$$

$$\alpha_\lambda(z) = \int_0^\infty \frac{dN}{dr} \pi r^2 Q_{ext} dr \quad 6$$

The respective efficiencies are dependent on size through the shape factor:

$$X_\lambda = \frac{2\pi r}{\lambda} \quad 7$$

and also on the particle composition as this effects the complex refractive index, and the shape. Note that within the particle ensemble described by the PSD each particle can be of a different composition and shape.

Given a particle of known specific shape, size and composition which is illuminated by a beam of specific power, polarization and wavelength it is a "relatively" straightforward procedure to determine the scattering and extinction properties, The inverse procedure, that is by analysing the scattered light field describe the particle or particles that are responsible for the scattering, is a much more difficult problem but it is the one that must be tackled here (Bohren and Huffman, 1998).

Instrument deployment and operations.

To maximise the potential return from the remote sensing instrumentation an optimal operational deployment scenario has to be developed. This scenario needs to be sufficiently flexible to meet the instrument capabilities of the two, IMO and NCAS, mobile laboratories.

Both laboratories have at their core, a ceilometer and a scanning Doppler lidar. The ceilometer operates at a wavelength of 905 nm and is configured to output:

- the height above the instrument of the bottom of up to 4 cloud layers
- profiles (height with respect to instrument) of range corrected attenuated aerosol backscatter coefficient:
  - maximum range: 10.235 km
  - range gate resolution: 5 m
  - number of gates: 2048
  - instrument averaging: 10 s

The Doppler lidars perform two function: 1) determination of the mean wind profile and 2) los (line of sight) profiles of range corrected attenuated aerosol backscatter coefficient. The operational wavelength is 1550 nm and can be configured to perform multiple types of scans: PPI and RHI. When not performing a designated scan the lidar will return to perform a vertical stare and it is only in the vertical stare position that data from the instrument channel sensitive to the cross polarised light can be accessed. In vertical stare the time between measurement points in the output file is determined by the number of "rays" making up the measurement. Increasing the number of rays in the measurement improves signal-to-noise ratio at the expense of temporal resolution. A ray is defined by the number of pulses it contains and for the NCAS lidar this is user configurable. The default is 1500 and as the laser prf (pulse repetition frequency) is 15 kHz this represents a pulse of approximately 1 second duration.

Measurement of the mean wind profile uses the following set up:

Azimuth Angles (AZ)	0˚, 90˚, 180˚, 270˚
Elevation Angle (EL)	90˚ (AZ = 0˚), 65˚ (AZ = 0˚, 90˚, 180˚, 270˚)
Pulses\ray	1500
Rays per measurement	5

There are two methods for determining the mean wind profile: Doppler Beam Swing (DBS) and Velocity-Azimuth Display (VAD). The DBS technique is computationally fast and makes use of a 5 point matrix inversion of the AZ, EL angle pairs (0˚, 90˚) (0˚, 65˚) (90˚, 65˚) (180˚, 65˚) and (270˚, 65˚). DBS however lacks the goodness-of-fit information as a measure for the reliability of the results that is provided by the VAD technique. With VAD a separate sine-wave is fitted at each height and the wind speed and direction determined from the amplitude, and offset (Weitkamp, 2005). It is the smoothness of the sine-wave fit that indicates the uncertainty in the retrieved wind speed and direct and this is effected by both instrument parameters and on turbulence.

For both techniques there also arises the question of representativity: the profile ultimately derived implies, implicitly, that it is a vertical profile directly above the instrument. The Doppler lidar measure los velocities and so to determine a mean wind speed and direction a combination of los velocities at different AZ and EL angles is required. The wind field being probed is not homogeneous so the measurement technique has to avoid biasing by either the vertical or horizontal component. To do this an AZ angle of 45˚ would be used, however at this angle the base diameter of the sample volume cone is approximately 14 km at the 10 km measurement limit of the beam. In other words the representativity error of the measurement increase with range and inversely with AZ. A balance is required between bias and representativity and this can be achieved with an AZ of 65˚ (base diameter of the sample volume cone is approximately 9 km at 10 km).

It should be noted that although the primary data required for wind is the los velocities the range corrected attenuated aerosol backscatter coefficient is also returned and can be used for particulate retrieval. The dedicated wind profiling scan will be executed every 10 minutes.

The limitation of the ceilometer is that, being vertically pointing, it only interrogates the atmospheric column directly above it and bearing in mind the pencil width diameter of the beam, this means having to be positioned directly beneath, for example, a cloud. To extract PSD information for a cloud (of any type) the laser light has to penetrate. The scattering action which provides the light that is measured also means power is lost form the main beam; this is attenuation. The greater the concentration of particulates in the path of the laser the greater the attenuation of the beam and this ultimately limits how far the instrument can "see".

After consultation with IMO and UKMO it has been recommended that these instruments are used to investigate the far field characteristics of an ash cloud as in this region the attenuation is far lower and a greater measurement range can be achieved. Practically this means that the RHI scan capability of the scanning lidar will need to be utilised. When considering suspended ash the RHI scan facility is again needed to counteract the problem that ash and lidar may not be co-located. To this end a series of RHI scans at AZ of 0˚, 45˚, 90˚, and 135˚ consisting of ELs of 0˚ - 180˚ (5˚ resolution) will be used. The EL range from 0˚ - 180˚ means that the scan goes through the vertical position and for ELs great than 90˚ this is equivalent to 0˚ - 90˚ scan with an AZ diametrically opposite; that is the implemented scan pattern is equivalent to AZ of 0˚, 45˚, 90˚, 135˚, 180˚, 225˚, 270˚, and 315˚ consisting of ELs of 0˚ - 90˚ (5˚ resolution). The pulses per ray will again be 1500 and the number of rays per measurement would again be 5 the maximum range is around 10km and the range gate resolution is 30 m. An RHI scan will be performed every 10 minutes.

When the lidar is not performing a scan the default action is to stare vertically and it in this position only that data from the depolarization channel can be accessed. The system cannot gather data from the two polarisation channels at the same time so switching occurs. The data is saved by the instrument in separate files and it should be noted that due to the channel switching, sample times are offset for these two streams. Scan scheduling is such that the RHI will run immediately after the winds scan completes. A fully documented standard operational procedure (SOP) for the implemented scanning regime is currently under development.

Retrieval Methodologies

At first sight it may seem that it is an impossible job to extract micro-physical information from the backscatter profiles but interest in this area is not confined to those interested in volcanic ash but is also of interest to the geophysical community as a whole. Being an ill-posed mathematical problem it is characterized by non-unique and highly unstable solutions arising from even small measurement or simulation errors. In practice, the solution of the ill-posed problem requires the introduction a priori information. A substantial body of work exists that explores a range of methodologies and are designed for the observational data available in this scenario.

For a technique to be applicable in the first instance it must make use of:

- pulsed rather than full wave lidar systems
- single laser wavelength

This is true of the ceilometers and for the scanning lidars when not performing a vertical dwell: operational scenario have to be considered and taken in to account. When performing a vertical dwell the scanning lidars can:

- use the depolarization channel.

The use of a sun-photometer, as with the NCAS mobile laboratory and the UKMO ceilometer network, and periodically with the IMO mobile laboratory does open up further techniques however it should be realised that provision of such a data stream is dependent on the availability of sunlight: an issue during the winter months at higher latitudes, and so will not be considered at this time (it is not ignored however).

The choice of method is thus restricted to the body of work that is immediately relevant: that is conforms\or can be adapted to the instrument operational parameters and allows retrieval of:

- particle size distribution as a function of range\altitude
- discrimination of particulate type between cloud, volcanic ash, dust, smoke, activated aerosol.
- characterize volcanic ash according to Marzano et al., 2011.

The primary method is the deployment of a forward operator\model as specific particulate properties such as radius and PSDs are not observed by either lidars or ceilometers. Several forward operators for atmospheric chemistry and NWP model evaluation exist; for example the Geisinger et al., 2017 forward model which estimates the attenuated backscatter from volcanic ash and clouds in the free troposphere using COSMO-ART over Germany and lidar\ceilometer data but omits the effect of backscatter from boundary layer aerosols. Another forward operator estimates backscatter from dust and sea salt with the ECMWF IFS using CALIOP data from the CALIPSO satellite (Morcrette et al., 2009). The Chan et al. (2016) forward operator for Lufft CHM15K ceilometer measurements estimates attenuated backscatter as a prognostic mass mixing ratio of different aerosol species from NWP, utilising either Mie or T-matrix calculation with fixed size distributions and growth factors for a set number of species. The Charlton-Perez et al. (2015) forward operator to estimate vertical profiles of β_m accounts for the effects of aerosols (using MURK; Clark et al. 2008), liquid cloud and rain. Initial testing at rural sites suggests the forward operator produced realistic β_m compared to β_o observed with Vaisala CL31 ceilometer (Charlton-Perez et al., 2015, 2016). However, this forward operator is effectively wavelength-independent, with a fixed scattering efficiency ($Q_{ext} = 2$), a value typically not suitable for aerosols. Although this forward operator only requires the total bulk mass mixing ratio as aerosol input, it does not speciate the aerosol, so that physical growth and scattering properties are assumed invariant between particles: the latter being a critical assumption given that these properties vary significantly between different aerosol species (Seinfeld and Pandis, 2016).

The forward operator developed by Warren et al., 2018, an extension to that developed in Charlton-Perez et al. (2015), takes the bulk particulate characteristics (mean dry particle radius and number concentration) as determined from the standard mass concentration (Claxton, 2013) and assuming a composition is grown until in equilibrium with the local moisture field, Q_{ext} is then calculated.

Of all the examples using forward modelling the one that shows the most promise is that developed by Mereu et al., 2018 for the estimation of volcanic ash particle size and concentration. Here they couple a polarimetric backscattering forward model with a Monte Carlo ash microphysical model and apply a maximum-likelihood statistical approach to refine the solution.

All the forward models above make use of look-up-tables of aerosol optical properties and all make assumptions regarding particle shape, composition and homogeneity of the ensemble. In the generation of the look-up-tables Gasteiger and Wiegner, 2018 have developed a tool, Modeled Optical Properties of enSeMbles of Aerosol Particles – MOPSMAP that delivers the optical properties of particulate ensembles. This tool is computationally fast even for complex aerosol populations as it uses pre-calculated single particle optical properties.

The scanning lidars operated by both NCAS and IMO also include the capability to measure the proportion of the backscattered light that is polarised: the light transmitted by the lidar is linearly polarised and when scattered the axis of polarisation can be either parallel to that of the incident light or perpendicular. At all scanning angle the lidars are able to determine the backscatter coefficient for the light with a polarisation axis parallel to that of the transmitted beam but can only do this for perpendicular polarisation when the instrument is looking directly upward. If operated in this fashion the perpendicular polarisation channel, also known as the cross channel provides additional input to a forward models but also opens an additional analysis path by way of the depolarisation ratio. The volume depolarisation ratio, δ, is defined as:

$$\delta = \frac{\beta_{\perp}}{\beta_{||}} \qquad 8$$

Zhou et al., 2013 have used the depolarization-attenuated backscatter relationship to successfully develop a method that allows for the distinction between water cloud and dust. Single scattering by water droplets does not depolarize backscattered light while multiple scattering events do tend to depolarize lidar signals within water cloud. The layer-integrated depolarization ratio of a water cloud shows quite large values which increase with layer-integrated attenuated backscatter coefficient. Polarization, however, is sensitive to non-spherical particles such as ice and dust. Donovan and Apituley, 2013 note that when limited to single-wavelength visible or ultraviolet backscatter lidar data, traditional approaches for estimating the aerosol extinction profile typically involve (either explicitly or implicitly by, e.g., choosing a reference range and a corresponding extinction boundary value) calibrating the lidar signal on a profile-by-profile basis. They develop a new technique for estimating optical backscatter and extinction profiles using the observed volume depolarization ratio and uncalibrated lidar backscatter signals. The depolarization calibration is not affected by laser power variations or variations in the near-field atmospheric transmittance and other such factors and so the relevant depolarization calibration does not have to be performed on a profile-by-profile basis leading to a retrieval based on the

depolarization ratio that is well suited to being applied in an automatic fashion. This technique was developed as a consequence of the ash cloud resulting from the Eyjafjallajökull eruption but has been extended for use in the determination of liquid-cloud microphysical properties (Donovan et al., 2015).

In the introduction we mentioned that in some circumstances sun-photometer measurements are available. Lopatin et al., 2013 introduce the GARRLiC algorithm (Generalized Aerosol Retrieval from Radiometer and Lidar Combined data) that simultaneously inverts coincident lidar and radiometer observations and derives a united set of aerosol parameters. Such synergetic retrieval results in additional enhancements in derived aerosol properties because the back-scattering observations by lidar improve sensitivity to the columnar properties of aerosol, while radiometric observations provide sufficient constraints on aerosol amount and type that are generally missing in lidar signals. This algorithm has been tuned for multi-wavelength elastic lidar but could, in principle be for use here. Of greater interest is LIRIC (on which GARRLiC is based), the lidar-radiometer inversion code developed in EARLINET (Chaikovsky et al., 2016). The LIRIC inversion algorithm can be divided into three key procedures: (i) parameterization of the object under study (i.e. development of the aerosol layer model); (ii) forward modelling, i.e. derivation of the equations that relate observed signals with specified parameters of the aerosol model; and (iii) inverse modelling or retrieval of the target parameters of the aerosol model that minimize discrepancies between the measured and the calculated input signals.

No one solution currently exists that can be picked up and deployed operationally, rather the best methodologies will have to be selected, adapted and tested in order to meet the needs outlined here. They are all dependent on some degree of forward modelling that requires the calculation of single particle optical properties. For volcanic ash the most comprehensive study is that of Vogel et al., 2017 which shows that the variance of the complex refractive indices in the wavelength range between λ = 300 nm and 1500 nm depends systematically on the composition of the samples: the real part varying from n = 1.38 to 1.66 depending on ash type and wavelength and the imaginary part from k = 0.00027 to 0.00268.

The overall methodology adopted will aim to exploit all the data available arising from the instruments deployed and the manner in which they are operated and this is shown in figure 1 below.

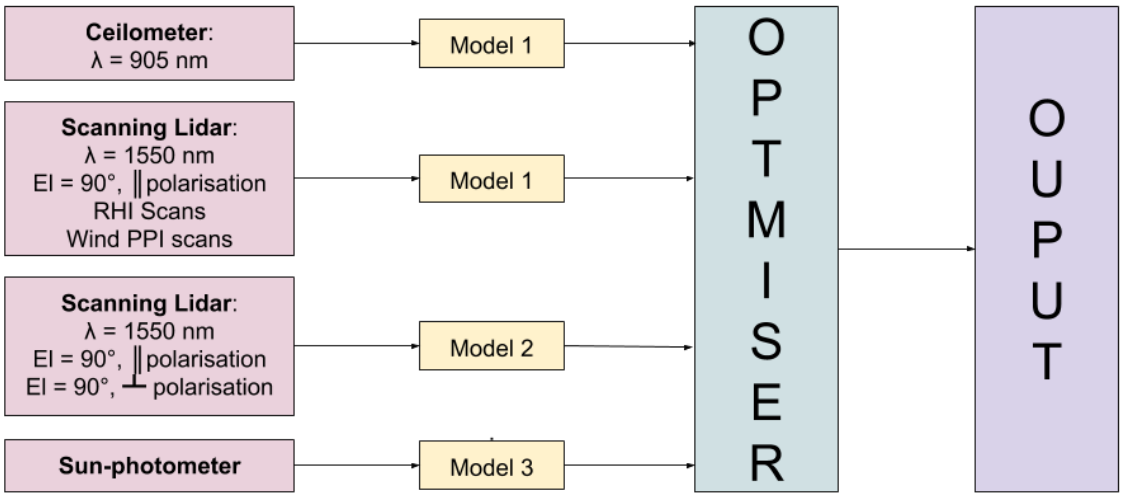

Figure 1: Schematic of the proposed hybrid methodology to be adapted. Each individual data stream will have an appropriate retrieval model developed: the operational output and uncertainty will be the result of an optimisation of the combined output streams in addition to the individual outputs. The aim is to provide sufficient information for the operational offices to make the best informed decision.

Figure 1 shows that three separate retrieval models are to be developed. Model 1 follows the methodologies based around a forward model that utilises a single laser wavelength, model 2 will be designed to make use of deplarisation and model 3 to make use of photometer data if and when available. Operationally the output variables and their associated uncertainties will be the result of an optimisation of the combined output streams: in addition to the individual model outputs. The aim is to provide sufficient information for the operational offices to make informed decision.

Results

The results presented in the following section are specific to model 1. Model 1 is the one that is applicable to the mode of operation that will provide the most continuous stream of data and its development is thus prioritised.

Figure 2 shows a provisional schematic of the proposed retrieval process and this is broken down into phases that correspond to distinct bodies of work: the phase ordering, 1 – 5 indicating the order in which they are to be tackled. Note Phase 6: Optimisation for Real Time Operations is not shown in figure 1 but will be essential long-term.

The outcome of this work is to produce a retrieval which provides operational meteorological services with an easy to use tool producing practical information (including uncertainty) in as close to real time as possible. What operational meteorological services consider to be the most use full output and the acceptable time delay has been determined through discussions held between NCAS, IMO, BGS (British Geological Service), and UKMO at the 6 monthly meeting of the Icelandic Volcanic MoU group: an international inter-agency group formed to facilitate improvements in the response capability and infrastructure resilience of UK and Iceland during volcanic eruptions and re-suspended ash\dust events.

In this section we will report on the progress of each phase and the rationale behind the approach taken.

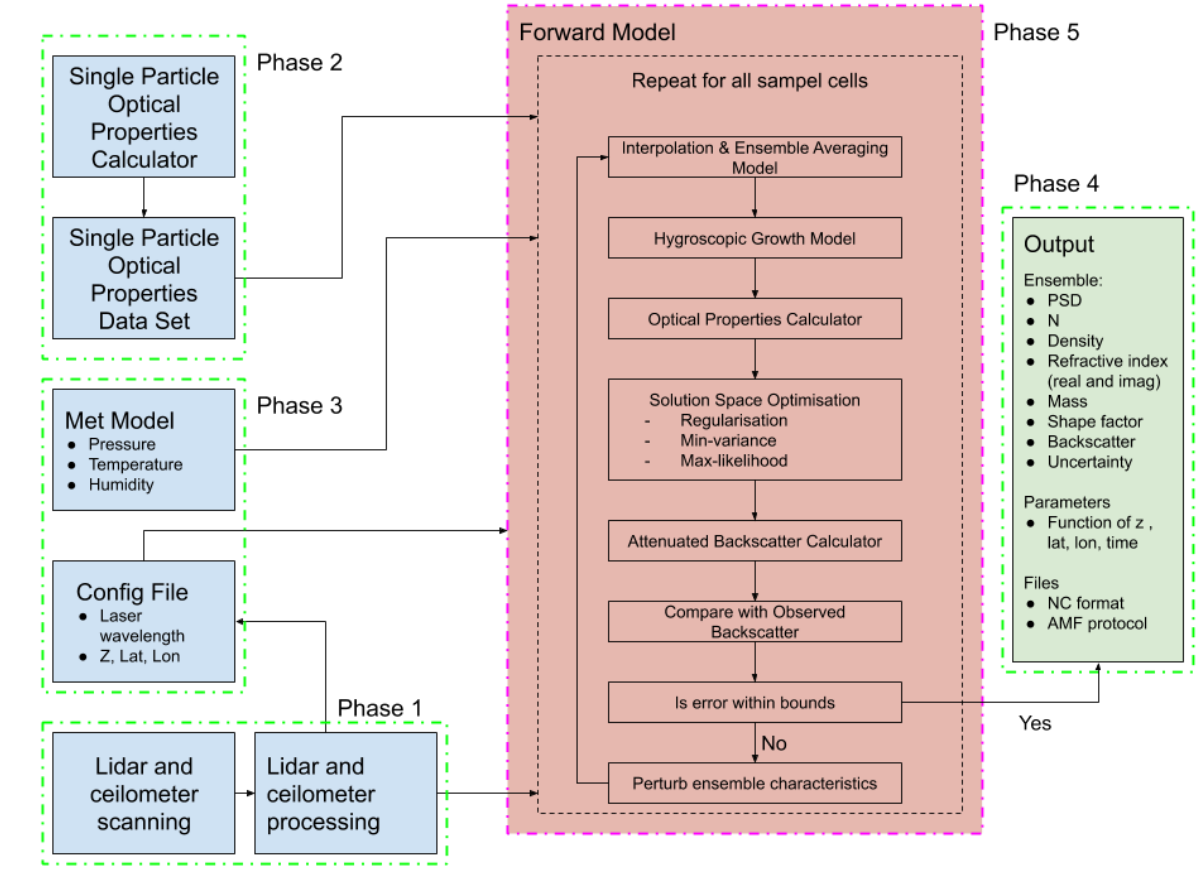

Figure 2: Schematic of Retrieval process

Phase 1: Processing General.

With a regularised scan regime universal processing code can be developed with the only instrument unique modules required being a parser that converts the output files from each instrument to a common format. The data processing has to provide instrument files for archiving and also files that can be passed to the forward model. Note that the data files from the two instruments will be kept separate as they operate at two different wavelengths and as such represent two separate instances of the forward model. The processing of data will be performed locally on a server in the observatory: this reduces the amount of data that has to be back hauled, and will occur every half hour.

Data processing also has to deliver data files that can be archived: the archive files being formatted that they are self-supporting containing meta data making them re-usable for further analysis decades in the future: that is the FAIR (Findable, Accessible, Interoperable, and Reusable) principles of open data will be implemented. Full details of this can be found at: https://www.force11.org/group/fairgroup/fairprinciples.

Archive data files from the NCAS instrumentation are required to be archived on the UK atmospheric data archive administered by CEDA (https://www.ceda.ac.uk/). There is no restriction on access to this data and this data should be available within one week of capture. An account on CEDA will be required in order to down load it. All archived NCAS data will follow the AMF Data Standard (cf-compliant) and full details of the principles and

the comprehensive details of the data products developed for a wide range of instruments including those to be used here can be found at: https://sites.google.com/ncas.ac.uk/ncasobservations/home/background.

Phase 1: Ceilometer - data processing and archiving

The raw ceilometer data will first be cleaned and quality controlled (QC) with QC flags added to indicate the "goodness" of the data. The process followed for cleaning and QC will be detailed in an SOP and this SOP is currently under development and is also applicable to all the NCAS ceilometers. The associated data product are cloud-base and aerosol-backscatter. In the case of the NCAS ceilometer it is this data that will be visualised as "Quick Looks" and disseminated via the data catalogue available on the dedicated Observatory website (under development). This website is open access and the Quick Looks publically available.

Once cleaned and QC'd the data will be averaged to a 5 minute time base centred on the 5 minute mark and as consequence the mean and standard deviation of the range corrected attenuated aerosol backscatter coefficient will be created: all times will be with respect to UTC derived from GPS. Each of these point will then be located in a 3D sample space by way of its altitude with respect to geoid WGS84 and its latitude and longitude again all derived from GPS. The data files containing the 5 minute data will also follow the same AMF Data Standard protocol as the archive files: an appropriate data product is under construction.

The ceilometer automatically identifies the base of layers and the ceilometer processing will compare with those identified using wavelet analysis (Brooks, 2003) of the profile: knowing where layers are is equally important as knowing the microphysical properties of the aerosol in the layer for dispersion models. This is currently under development. Quick looks showing this comparison will again be made available via the data catalogue.

A three documented SOP for ceilometer processing, visualisation, and archiving is currently under development. The data processing path is shown schematically in figure 3 below:

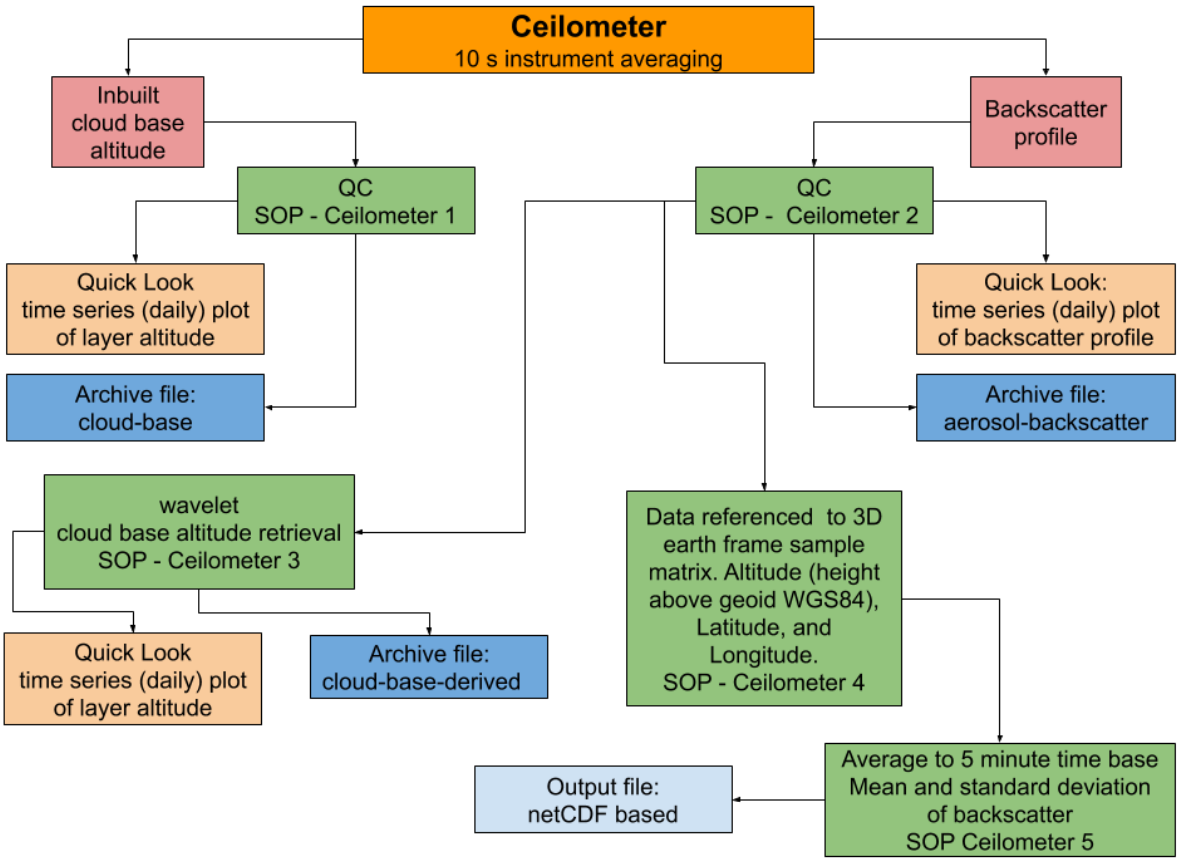

Figure 3: Schematic of proposed ceilometer processing.

Phase 1: Lidar - data processing and archiving

The data processing required to deliver the mean wind profiles will not be discussed in any more detail than to say that profiles derived using both VAD and DBS will be delivered and archived. The appropriate data product is currently being developed following the AMF Data Standard and as with the 10s ceilometer data will be archived and accessed through CEDA. Quick Looks from both techniques will be presented on the website. A documented SOP for the delivery of winds using the two techniques is also currently under development.

The wind scan, RHI, and stare data (including the depolarization channel if activated) will be quality controlled including the enhanced background correction developed by Maninnen et al., (2106) and archived following the SOP developed for operation of identical AMF instruments. It is this data that will be used to generate "Quick Looks" for the website

Additional processing is required to produce files that can be ingested into the forward model. Like the ceilometer these files will follow the same AMF Data Standard protocol as the archive files. A 3D sample space will be initialised that is defined in terms of altitude, latitude and longitude. Backscatter data from the scans and vertical stare can be located in the earth frame this 3d sample space represents, by virtue of GPS height (height above geoid WGS84) and position of the instrument, the AZ and EL angles of a scan which are relative to the instrument and the distance from the instrument of the range gate boundaries. Considering a period of 10 mins, centred on the 10 minute mark, data can be attributed (in whole or in part) to an earth frame sample bin. The contents of each bin will be averaged and an uncertainty (standard deviation) determined. The data files containing the 10 minute data will follow the same AMF Data Standard protocol as the archive files. A documented SOP is currently under development.

As with the ceilometer the lidar can be used to identify layers and the same processing can be applied to the above matrix to provide a map of the layers that are visible to the lidar. Again a documented SOP is currently under development.

Figure 4 shows the data processing pathway schematically.

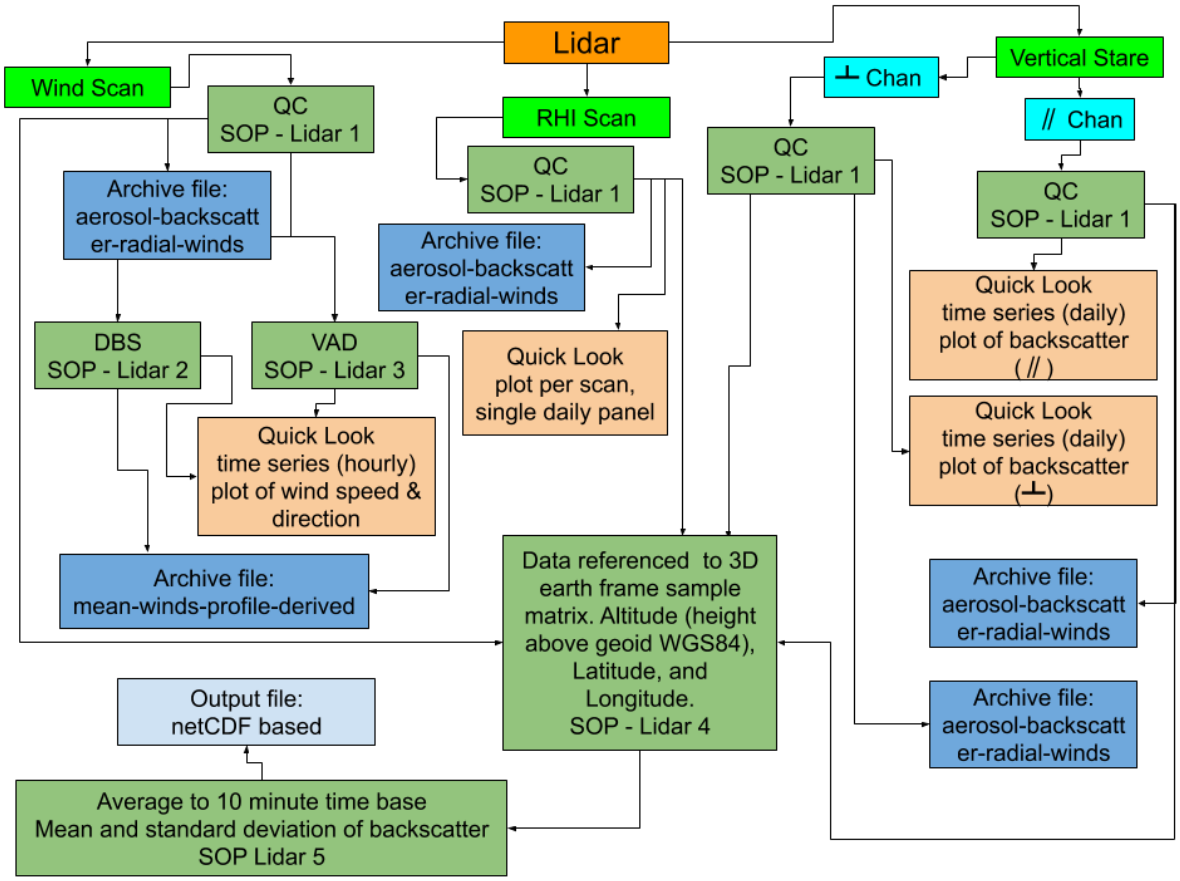

Figure 4. Schematic of the lidar processing pathway.

Phase 2: Single Particle Optical Properties

As part of the development of MOPSMAP (Gasteiger and Wiegner, 2018) a data base of single particle optical properties has been made available in the form of netCDF files in addition to associated fortran codes (https://zenodo.org/record/1284217#.XZdNWlVKjd9). Retrieval model 1 is centred on this the methodology and tables 1 and 2 of Gasteiger and Wiegner, (2018) show the parameter range used by the authors in the development of their data set. Attention should be drawn the use of the size parameter x. Using the size parameter removes the need to have a data set appropriate for a particular instrument, the lidar and ceiloeter having different laser wavelengths. The laser wavelength also comes in to play through the refractive index and the range of real and imaginary refractive indices used is based on mineral dust properties presented by Gasteiger et al., (2011). Vogel

et al., (2017) have developed a reference data set specifically regarding the physiochemical and optical properties of volcanic ash and this will require integrating in to the dataset to be used here. To this end it has been decided to generate a new and extended data set from first principles, following the protocols of Gasteiger and Wiegner, 2018, but including ash and extending, in both range and resolution, size parameter, and particle shape. The Mie, T-Matrix, Improved Geometric Optics, and Discrete Dipole Approximation codes referenced by Gasteiger and Wiegner, 2018 will be ported to python, parallelized and run on JASMIN (http://www.jasmin.ac.uk/what-is-jasmin/): a UK "super-data-cluster" which delivers infrastructure for data analysis.

The code porting and development is currently in progress and once complete a series of test files matching the input parameter of Gasteiger and Wiegner, 2018 will be produced and be compared to those made available with MOPSMAP tool. Only once the files produced by the ported code match those in MOPSMAP will the generation of the extended data set begin.

Phase 3: Auxiliary Data

This module will acquire pressure (P), temperature (T), and humidity (U) data and place it on the same tempo-spatial grid as the lidar and ceilometer measurements. It is anticipated that ECMWF and GSF data streams will be used in conjunction with WRF model data (and instance of WRF is run by NCAS specifically for Iceland). The co-ordinate space defined by this data will not match that of the instruments so interpolation and nearest neighbour choice will be adopted to provide the atmospheric thermo-dynamic map matching the measurement map. This data is required in order to account for the hydroscopic growth of the hypothesised aerosol ensemble, the optical properties of which will be compared to measurements.

The configuration file will be designed to pass the required initialisation parameters to the forward model. In addition to the thermo-dynamic state of the atmosphere the information required is the laser wavelength of the instrument and a flag to indicate if operating in an eruption scenario. If this latter flag is set it will be assumed that ash dominates that hypothetical aerosol ensemble, the only other constitute considered in the eruption scenario being water.

This phase is at the concept stage.

Phase 4: Output Module

This module is designed to take the anticipated wide range of data products produced by the forward model module when it exits the run loop as well as those form the layer analysis and deliver two products: one containing parameters for the dispersion models and one for archiving. These files will be netCDF and follow the AMF Data Standard protocol. No work will start on this phase until phases 1 – 3 and 5 have been completed and tested. This phase will require extensive end user input and this will be obtained through consultation with the IMO and UKMO operational offices as well as London VAAC.

Phase 5: Forward model

This is the main module and work has begun to set up the computational environment. Work will start on it development once phase 1 – 3 have been completed.

Phase 6: Optimisation for Real Time Operations

No work will start on this phase until phases 1 – 5 have been completed and tested.

Meetings

The main meeting required to support this body of work involve the individuals who participate in the Icelandic Volcano MoU. As such the use is made of the virtual meeting held annually in March and the face-to-face held annually in September to discuss progress and acquire end user requirements.

References

Bohren C. F, and D. R. Huffman, 1998: *Absorption and Scattering of Light by Small Particles.* John Wiley & Sons Inc., New York.

Brooks, I. M., 2003: *Finding boundary layer top: Application of a wavelet covariance transform to lidar backscatter profiles.* Journal of Atmospheric and Oceanic Technology, 20 (8). 1092 - 1105. ISSN 0739-0572

Chaikovsky A., O. Dubovik, B. Holben, A. Bril, P. Goloub, D. Tanré, G. Pappalardo, U. Wandinger, L. Chaikovskaya, S. Denisov, J. Grudo, A. Lopatin, Y. Karol, T. Lapyonok, V. Amiridis, A. Ansmann, A. Apituley, L. Allados-Arboledas, I. Binietoglou, A. Boselli, G. D'Amico, V. Freudenthaler, D. Giles, M. J. Granados-Muñoz, P. Kokkalis, D. Nicolae, S. Oshchepkov, A. Papayannis, M. R. Perrone, A. Pietruczuk, F. Rocadenbosch, M. Sicard, I. Slutsker, C. Talianu, F. De Tomasi, A. Tsekeri, J. Wagner, and X. Wang, 2016: *Lidar-Radiometer Inversion Code (LIRIC) for the retrieval of vertical aerosol properties from combined lidar/radiometer data: development and distribution in EARLINET*. Atmos. Meas. Tech., 9, 1181–1205, doi:10.5194/amt-9-1181-2016.

Chan, K.L., M. Wiegner, H. Flentje, I. Mattis, F. Wagner, J. Gasteiger, A. Geiß: 2016. *Simulation of ceilometer backscatter signal from global chemical transport model data*. 2016-12-01 SWG 1.4: O-B Analysis for Ceilometers. Paris, France.

Charlton-Perez, C., E, O'Connor, S. Ballard, M. Adam, D. Klugmann, O. Cox: 2015. *Review of ceilometer operator design*. Met Office

Charlton-Perez, C., D. Simonin, S. Ballard, E. Hopkin, A. Illingworth, S. Kotthaus, C. Westbrook, C. S. B. Grimmond: 2016. *Suitability of Ceilometer Observations for DA, Data Assimilation and Ensembles Science*. Report 10. Met Office.

Clark, P.A., S. A. Harcourt, B. Macpherson, C. T. Mathinson, S. Cusak, M. Naylor: 2008. *Prediction of visibility and aerosol within the operational Met Office Unified Model. I: Model formulation and variational assimilation*. Q. J. R. Meteorol. Soc. 134, 1801–1816, doi:10.1002/qj

Claxon B. M., 2013: *Parameters Concrolling the Aerosol Hydration Scheme within the UKV Visibility Paramaterization.* vol 85. Met Off. Cardingt. Tech, 1 – 35.

Costa, A., G. Macedonio, A. Folch, 2006*: A three-dimensional Eulerian model for transport and deposition of volcanic ashes*. Earth Planet. Sci. Lett., 241 (3-4), 634-647.

Donovan D. and A. Apituley, 2013*: Practical depolarization-ratio-based inversion procedure: lidar measurements of the Eyjafjallajökull ash cloud over the Netherlands.* Applied Optics, 52, 11, 2394 – 2415, doi:10.1364/AO.52.002394

Donovan D. P., H. Klein Baltink, J. S. Henzing, S. R. de Roode, and A. P. Siebesma, 2015: *A depolarisation lidar-based method for the determination of liquid-cloud microphysical properties.* Atmos. Meas. Tech., 8, 237–266, doi:10.5194/amt-8-237-2015

Geisinger A., A. Behrendt, V. Wulfmeyer, J. Strohbach, J. Förstner, and R. Potthast, 2017: *Development and application of a backscatter lidar forward operator for quantitative validation of aerosol dispersion models and future data assimilation.* Atmos. Mease, Tech., 10, 4705 – 4726, doi:10.5194/amt-10-4705-2017.

Jones A.R., D. J. Thomson, M. Hort and B. Devenish, 2007: *'The U.K. Met Office's next-generation atmospheric dispersion model, NAME III'*, in Borrego C. and Norman A.-L. (Eds) Air Pollution Modeling and its Application XVII (Proceedings of the 27th NATO/CCMS International Technical Meeting on Air Pollution Modelling and its Application), Springer, pp. 580-589, 2007.

Gasteiger J., M. Wiegner, S. Groß, V. Freudenthaler, C.Toledano, M. Tesche, and K. Kandler, 2011: *Modelling lidar-relevant optical properties of complex mineral dust aerosols.* Tellus B: Chemical and Physical Meteorology, 63:4, 725-741, doi:10.1111/j.1600-0889.2011.00559.x

Gasteiger J. and M. Wiegner, 2018: *MOPSMAP v1.0: a versatile tool for the modelling of aerosol optical properties.* Geosci. Model Dev., 11, 2739 – 2762, doi:10.5194/gmd-11-2739-2018.

Kovlev V. A. and W. E. Eichinger, 2004: *Elastic Lidar.* John Wiley & Sons Inc., New York.

Lopatin A., O. Dubovik, A. Chaikovsky, P. Goloub, T. Lapyonok, D. Tanré, and P. Litvinov: 2013. *Enhancement of aerosol characterization using synergy of lidar and sun-photometer coincident observations: the GARRLiC algorithm.* Atmos. Meas. Tech., 6, 2065–2088, doi:10.5194/amt-6-2065-2013

Manninen A. J., E. J. O'Connor, V. Vakkari, and T. Petäjä, 2106: *A generalised background correction algorithm for a Halo Doppler lidar and its application to data from Finland*. Atmos. Meas. Tech., 9, 817–827. doi:10.5194/amt-9-817-2016.

Marzano F. S., E.Picciotti, G. Vulpiani, and M. Montopoli, 2011: *Synthetic Signatures of volcanic ash cloud particles from X-band dual-polarization radar.* IEEE Trans. Geosci. Remote Sens., 50, 1, 193 – 211, doi:10.1109/TGRS.2011.2159225.

Mereu L., S. Scollo, S. Mori, G. Leto, and F. S. Marzano, 2018: *Maximum-Likelihood Retrieval of Volcanic Ash Concentration and Particle Size From Ground-Based Scanning Lidar*. IEEE Transactions on Geoscience and Remote Sensing (Volume: 56, Issue: 10, Oct. 2018), doi:10.1109/TGRS.2018.2826839.

Morcrette, J.-J., O. Boucher, L. Jones, D. Salmond, P. Bechtold, A. Beljaars, A. Benedetti, A. Bonet, J. W. Kaiser, M. Razinger, M. Schulz, S. Serrar, A. J. Simmons, M. Sofiev, M. Suttie, A. M. Tompkins, A. Untch: 2009. *Aerosol analysis and forecast* in the European Centre for Medium-Range Weather Forecasts Integrated Forecast System: Forward modeling. J. Geophys. Res. 114, D06206, doi:10.1029/2008JD011235

Omar A. H., D.M. Winker, C. Kittaka, M. A. Vaughan, Z. Liu, Y. Hu, C. R. Trepte, R. R. Rogers, R. A. Ferrare, K-P. Lee , R. E. Kuehn, C. A. Hostetler, 2009: *The CALIPSO Automated Aerosol Classification and Lidar Ratio*

Selection Algorithm. Journal of Atmospheric and Oceanic Technology (Volume 26), doi:10.1175/2009JTECHA1231.1.

Seinfeld, J.H., Pandis, S.N., 2016. Atmospheric Chemistry and Physics: From Air Pollution to Climate Change. Wiley, Haboken.

Stein A, R. R. Draxler, G. Rolph, B. J. B. Stunder, M. D. Cohen, F. Ngan, 2016: *NOAA's HYSPLIT atmospheric transport and dispersion modeling system*. Bulletin of the American Meteorological Society. 96. 150504130527006, doi:10.1175/BAMS-D-14-00110.1.

van de Hulst H. C., 1981: *Light Scattering by Small Particles.* John Wiley & Sons Inc., New York.
Vogel A., S. Diplas, A. J. Durant, A. S. Azar, M. F. Sunding, W. I. Rose, A. Sytchkova, C. Bonadonna, K. Krüger, and A. Stohl, 2017: *Reference data set of volcanic ash physicochemicaland optical properties.* J. Geophys. Res. Atmos., 122, 9485–9514, doi:10.1002/2016JD026328.

Vogel A., S. Diplas, A. J. Durant, A. S. Azar, M. F. Sunding, W. I. Rose, A. Sytchkova, C. Bonadonna, K. Krüger, and A. Stohl, 2017: *Reference data set of volcanic ash physicochemical and optical properties*. J. Geophys. Res.Atmos.,122, 9485–9514, doi:10.1002/2016JD026328.

Warren E., C. Charlton-Perez, S. Kotthaus, H. Lean, S. Ballard, E. Hopkin, S. Grimmond: 2018: *Evaluation of forward-modelled attenuated backscatter using an urban ceilometer network in London under clear-sky conditions.* Atmospheric Environment, 191, 532 – 547, doi:10.1016/j.atmosenv.2018.04.045

Weitkamp C., 2005: *Lidar: Range-Resolved Optical Remote Sensing of the Atmosphere.* Springer Science +Business Media Inc., New York.

Zhou T., H. Jianping, H. Zhongwei, L. Jingjing, W. Wencai, and L. Lei, 2013: *The depolarization–attenuated backscatter relationship for dust plumes.* Optics Express, 21, 13, 15195 – 15204, doi:10.1364/OE.21.015195